Inorganic Chemistry
Cite This: Inorg. Chem. 2019, 58, 8633−8644
Article
pubs.acs.org/IC

Highly Efficient N-Pivot Tripodal Diglycolamide Ligands for Trivalent f-Cations: Synthesis, Extraction, Spectroscopy, and Density Functional Theory Studies

Seraj A. Ansari,[†] Prasanta K. Mohapatra,*[,†] Andrea Leoncini,[‡] Sk. Musharaf Ali,[§] Jurriaan Huskens,[‡] and Willem Verboom*[,‡]

[†]Radiochemistry Division, Bhabha Atomic Research Centre, Trombay, Mumbai 400085, India

[‡]Laboratory of Molecular Nanofabrication, MESA+ Institute for Nanotechnology, University of Twente, P.O. Box 217, 7500 AE Enschede, The Netherlands

[§]Chemical Engineering Division, Bhabha Atomic Research Centre, Mumbai 400085, India

Supporting Information

ABSTRACT: A series of four N-pivot tripodal diglycolamide (DGA) ligands, where three DGA moieties are attached to the central N atom via spacers of different lengths and with varying alkyl substituents on the amidic nitrogen of DGA ($\mathbf{L_I}$–$\mathbf{L_{IV}}$), were studied for their extraction and complexation ability toward trivalent lanthanide/actinide ions, including solvent extraction, complexation using spectrophotometric titrations, and luminescence spectroscopic studies. Introduction of a methyl group on the amidic nitrogen atom gives rise to a 400 fold increase of the Eu distribution (D) value [$\mathbf{L_{III}}$ (NMe) vs $\mathbf{L_{II}}$ (NH)] at 1 M HNO_3. Enlargement of the spacer length between the pivotal N atom and the DGA moieties with one carbon atom results in a 14 times higher D_{Eu} value [$\mathbf{L_I}$ (C3) vs $\mathbf{L_{II}}$ (C2)]. Slope analyses showed that Eu^{3+} was extracted as a bis-solvated species with all four ligands. The compositions of the Eu^{3+}/L complexes were further confirmed by spectroscopic measurements, its formation constants following the order: $\mathbf{L_{III}} > \mathbf{L_{IV}} > \mathbf{L_I} > \mathbf{L_{II}}$. Luminescence spectroscopy and electrospray ionization mass spectrometry revealed that all four ligands form $[Eu(L)_2(NO_3)_3]$ complexes. Density functional theory and thermodynamic parameters corroborated the existence of $[Eu(L)_2(NO_3)_3]$ complexes.

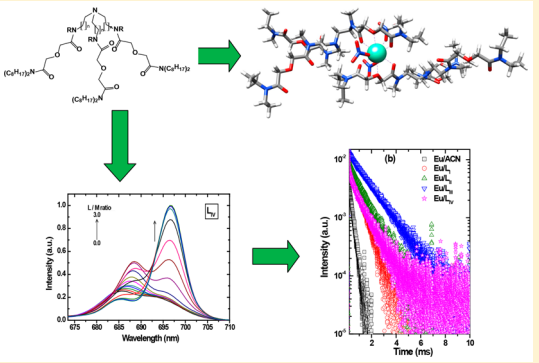

INTRODUCTION

During last few decades, the diglycolamide (DGA)[1] class of ligands has emerged to be the most effective extractants for the separation of trivalent actinides and lanthanides from high level liquid waste (HLLW) in the proposed "actinide partitioning" program.[2] DGA ligands are known to show preference for trivalent actinide/lanthanide ions over the hexavalent UO_2^{2+} cation, which is not the case for other ligands proposed for actinide partitioning such as carbamoylmethylene phosphineoxide (CMPO)[3] and malonamides.[4] The higher affinity for trivalent actinides over UO_2^{2+} cation was assigned to the formation of molecular aggregates through reverse micelle formation,[5] which shows a higher affinity to the former cations than the latter due to the presence of two equatorial oxygen atoms. Several fundamental complexation studies,[6] including crystal structures[7] and EXAFS studies,[8] indicated the coordination of three DGA ligands with Eu^{3+}/Am^{3+} via all three donor oxygen atoms of these ligands. On the basis of the *N,N,N′,N′*-tetraoctyl diglycolamide (TODGA) aggregate formation[5a] being the sole reason for the reversal in the extraction trend, it is clear that three to four TODGA molecules are associated in the formation of a reverse micelle in nonpolar diluents such as *n*-dodecane when contacted with dilute nitric acid. The core of such a reverse micelle shows preferential affinity for trivalent actinides (also for lanthanides) in a size-selective manner.[9] Taking the clue from this, it was predicted that preorganization of 3−4 DGA molecules on a molecular platform would enhance the affinity of these ligands for trivalent f-cations. It is evident from several studies that the extraction of lanthanide and actinide ions increases several fold upon functionalizing the DGA moieties onto a multipodal platform giving tripodal diglycolamides (T-DGAs),[10] DGA-functionalized calix[4]arenes,[11] or DGA-functionalized pillar[5]arenes.[12] Such preorganized ligands not only show a higher extraction ability for trivalent actinides but also give a better selectivity over uranium and strontium desired for the proposed "actinide partitioning" strategy.

Recent studies on a novel N-pivot tripodal DGA, TREN-DGA ($\mathbf{L_{II}}$; Figure 1) revealed a promising extraction ability toward trivalent actinides and lanthanides over UO_2^{2+}, Cs^+, and Sr^{2+}.[13] The ligand was also studied in a supported liquid

Received: April 4, 2019
Published: June 10, 2019

DOI: 10.1021/acs.inorgchem.9b00985
Inorg. Chem. 2019, 58, 8633−8644

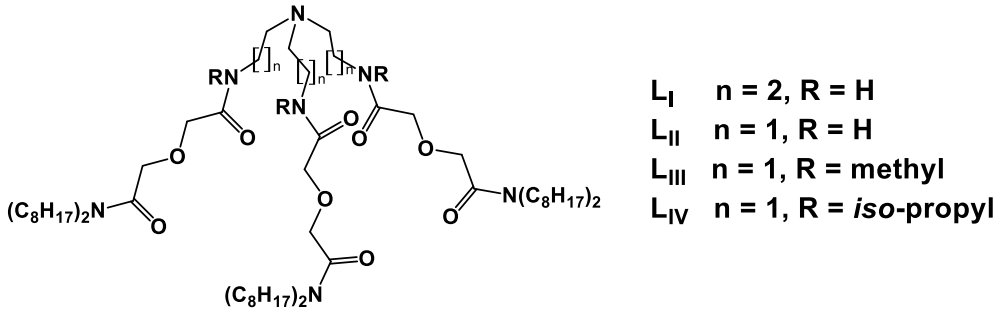

Figure 1. Structural formulas of the ligands used in the present study.

membrane for preferential transport of trivalent lanthanides and actinides over uranyl ions[13b] and for making a PVC-based potentiometric sensor.[13c] However, a detailed investigation on the metal/ligand interactions as quantified by the determination of complex formation constants is lacking. Furthermore, the effect of various *N*-alkyl substituents on the complexation ability of these ligands is not understood.

The present study was, therefore, undertaken for in-depth understanding of the complexation of these ligands with trivalent f-elements. In the present work, a series of four N-pivot tripodal diglycolamide ligands (L_I–L_{IV}; Figure 1) were synthesized, and their complexation ability toward trivalent lanthanide/actinide ions was studied. Emphasis was made to understand the effects of (i) the number of spacer atoms between the central N atom of the tripodal platform and the DGA unit, and (ii) alkyl substituents on the amidic nitrogen of the DGA moieties. Solvent extraction studies were performed in 5% isodecanol/*n*-dodecane, whereas Eu^{3+}/ligand optical spectroscopic single phase titrations were carried out in acetonitrile medium. The complexes were identified by electrospray ionization mass spectrometry (ESI-MS). Additionally, complexation of all the four ligands with Eu^{3+} ion was studied by density functional theory (DFT) calculations to understand the bonding and to determine the interaction energies.

RESULTS AND DISCUSSION

Preparation of Ligands. Ligand L_I was prepared in 64% yield by reaction of the commercially available tris(2-aminopropyl)amine as a scaffold with 4-nitrophenyl 2-(2-(dioctylamino)-2-oxoethoxy)acetate in refluxing toluene (Scheme 1) in analogy to the previously reported ligand L_{II}.[13a] Upon completion of the reaction, in the ^{1}H NMR spectrum the signals of the DGA CH_2 protons shift from 4.57 (s) and 4.37 (s) ppm of the *p*-nitrophenyl-activated DGA to 4.22 (s) and 4.03 (s) ppm of L_{II}. The appearance of a triplet at 7.80 ppm highlights the formation of the amide groups. In a similar way, ligands L_{III} and L_{IV}, bearing methyl and isopropyl substituents, respectively (Figure 1), were prepared starting from tris(triaminoethyl)amine as a molecular platform in 76 and 92% yield, respectively.

Scheme 1. Synthesis of the N-Pivot Tripodal Diglycolamides L_I–L_{IV}

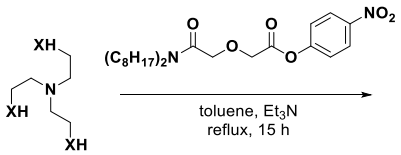

L_I	X = CH_2NH	64%
L_{II}	X = NH	73%
L_{III}	X = NMe	76%
L_{IV}	X = N(iPr)	92%

The ^{1}H NMR spectrum of ligand L_{III} is characterized by a group of signals at 2.99 and 2.95 ppm, belonging to the methyl groups. Because of the hindered rotation around the N–$C_{carbonyl}$ bond, the two possible rotamers of the amide group due to cis-trans isomerism are expected to be distinguishable in the ^{1}H NMR spectrum. The ligand exists, therefore, as a mixture of four different isomers, with zero, one, two, or three amide groups in which the C═O bond is pointing opposite to the N–Me group. The signals at 2.99 and 2.95 ppm can then be explained as the overlap of the peaks belonging to the four isomers. The presence of two distinct groups of signals in a 2:1 ratio, however, suggests that the peaks of the methyl groups of the four isomers are clustered according to their orientation with respect to the C═O group and that 2:1 is also the ratio between the two amide rotamers. The shape of the peaks around 4.3 and 2.7 ppm can be interpreted in a similar way, even though the separation between the signals is not as clear as for the CH_3 signals. In addition, the ^{13}C NMR spectrum also reflects a mixture of isomers, showing six additional signals than otherwise expected. A similar behavior is observed in the ^{1}H NMR spectrum of ligand L_{IV}, which also exists as a mixture of four isomers. In addition to a new multiplet at 1.21–1.16 ppm belonging to the methyl groups of the isopropyl group, the spectrum is characterized by the presence of two heptets at 4.52 and 3.97 ppm in a 1:3 ratio that belong to the CH of the isopropyl substituent, probably reflecting the ratio between the two rotamers of the amide moiety. The signals at 4.29 and 2.70 ppm are compatible with the presence of a mixture of isomers.

Extraction Studies. The liquid–liquid extraction data for Am^{3+} and Eu^{3+} from varying nitric acid solutions with all the four ligands are presented in Figure 2. The important inference that can be drawn from the data is that, for all the ligands, extraction of Eu^{3+} is always higher than that of Am^{3+}. This is a unique feature of DGA ligands studied for extraction of lanthanides and actinides, where extraction of Eu^{3+} is higher than that of Am^{3+}.[14] The separation factor between Eu^{3+} over Am^{3+} with the widely studied DGA ligand TODGA has been found to be as high as 10.[15] One might expect more interaction of the present ligands with the soft Am^{3+} cation due to the presence of the soft N atom at the center. However, looking at the extraction data, such possibility is ruled out as the N atom is probably not participating in bonding, and only provides a center to organize the three DGA moieties on the tripodal platform. As evident from Figure 2, the extraction of both Eu^{3+} and Am^{3+} increased monotonously with feed acidity implying that a

DOI: 10.1021/acs.inorgchem.9b00985
Inorg. Chem. 2019, 58, 8633–8644

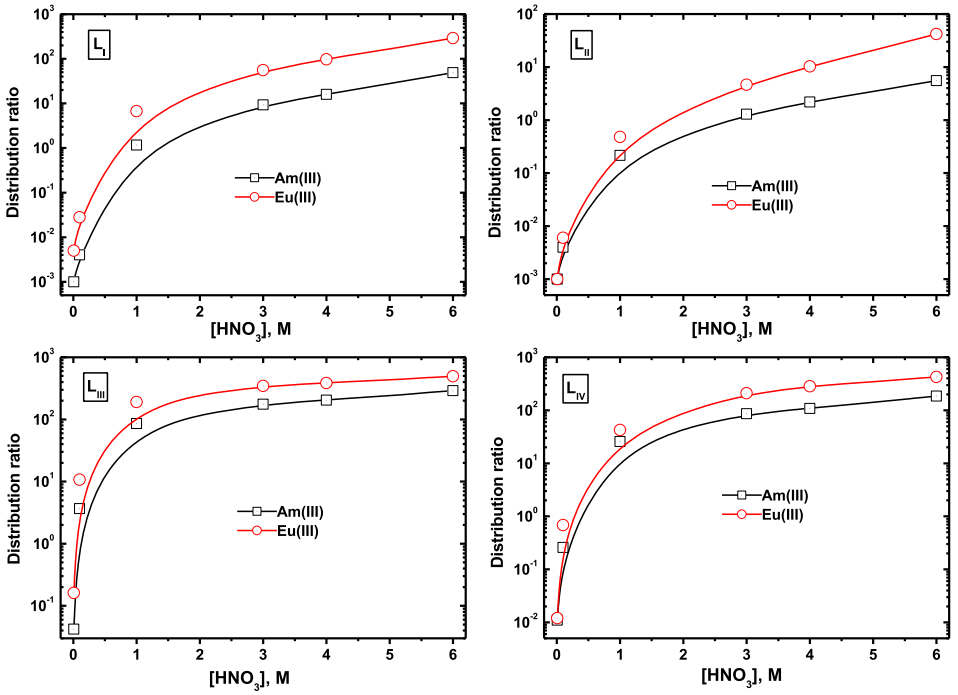

Figure 2. Distribution ratios of Am^{3+} and Eu^{3+} with DGA ligands $\mathbf{L_I}$–$\mathbf{L_{IV}}$. Organic phase: 1 mmol/L ligands in 5% isodecanol/*n*-dodecane. Temperature: 25 °C.

"solvation extraction mechanism" is being followed for all the four ligands. This mechanism is well established for neutral ligands, including the widely studied TODGA, where the extraction is explained by the following equilibrium reaction:

$$M^{3+}_{(aq)} + 3NO_3^-{}_{(aq)} + jL_{(org)} \overset{K_{ex}}{\rightleftharpoons} [M(NO_3)_3 \cdot jL]_{(org)} \quad (1)$$

where M^{3+} represents the Am^{3+} or Eu^{3+} ions, L is the neutral ligand, *i* and *j* represents the number of ligand molecules associated in the extracted complex. The subscripts (aq) and (org) represent the aqueous and organic phases, respectively. The equilibrium constant for the above reaction can be written as

$$K_{ex} = \frac{[M(NO_3)_3 \cdot jL]_{(org)}}{[M^{3+}]_{(aq)} \cdot [NO_3^-]^3_{(aq)} \cdot [L]^j_{(org)}} \quad (2)$$

where K_{ex} is the equilibrium constant referred to as extraction constant. The major difference between TODGA and the present set of ligands is that the *D* value of Am(III) is expected to be significantly lower (<0.01) for the former at 1 mM ligand concentration at 3 M HNO_3, indicating a significant improvement in these tripodal ligands which could be attributed to their preorganized nature. It can be also mentioned here that TODGA invariably formed 1:3 complexes with lanthanides,[16] while the present set of ligands formed 1:2 complexes and as will be discussed below involved only one DGA arm from each of the tripodal ligands.

Since the distribution ratio (*D*) is experimentally obtained as the ratio of the total metal ion concentration in the organic phase to that of in the aqueous phase, eq 2 can be simplified to

$$D = K_{ex} \cdot [NO_3^-]^3_{(aq)} \cdot [L]^j_{(org)} \quad (3)$$

An important feature of eq 3 is that it can be used to predict the composition of the extracted complex by the slope analysis. These studies involved experiments with Eu(III) as a representative of trivalent actinide/lanthanide ions. Additionally, as the complexation studies were carried out with Eu(III), it was pertinent to carry out these studies with the lanthanide ion. As shown in Figure 3a, the log–log plot of D_{Eu} vs ligand

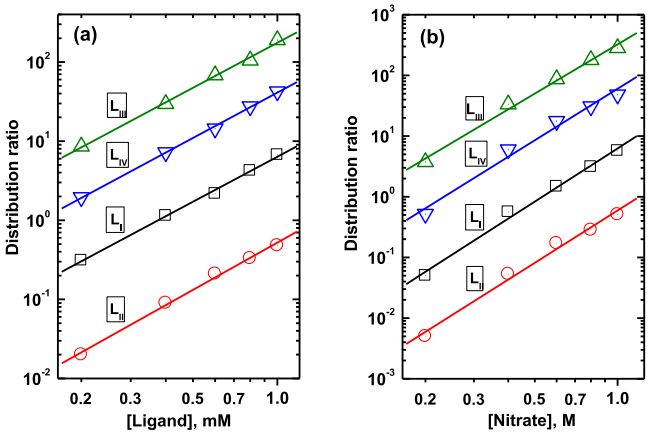

Figure 3. (a) Variation of D_{Eu} with ligand concentration at 1 M HNO_3. (b) Variation of D_{Eu} by 1 mmol/L ligand with nitrate concentration. Aqueous phase: 0.1 M HNO_3 + $NaNO_3$.

concentration at constant nitrate concentration (1 M HNO_3) yielded a slope value of ca. 2 for all ligands (Table 1). Similarly, the log–log plot of D_{Eu} vs nitrate ion concentration at constant ligand concentration (1 mmol/L) yielded a slope value of ca. 3 for all ligands (Figure 3b). One may expect a 1:1 metal to ligand stoichiometry for all the four ligands as nine O atoms from three DGA moieties of each ligand may bind with the Eu^{3+} in a tridentate manner to complete the coordination

DOI: 10.1021/acs.inorgchem.9b00985
Inorg. Chem. 2019, 58, 8633–8644

Table 1. Distribution Behaviour of Eu^{3+} Using Ligands L_I–L_{IV} at 1 M HNO_3

ligand	D_{Eu}	slope = j	slope = i
L_I	6.71 ± 0.34	1.89 ± 0.07	2.91 ± 0.14
L_{II}	0.48 ± 0.05	1.99 ± 0.06	2.86 ± 0.18
L_{III}	190 ± 17	1.89 ± 0.09	2.69 ± 0.13
L_{IV}	42.4 ± 2.4	1.90 ± 0.04	2.82 ± 0.21

requirement.[17] However, coordination of all the three DGA arms of the same ligand could be unfavored due to steric considerations. In view of the results obtained, one may come up with two possibilities. In the first case, out of the two ligands, one DGA unit from one ligand and two DGA units from another ligand may bind in a tridentate manner, thus completing the coordination requirement of the Eu^{3+} ion. In such a case, three nitrates shall remain in the secondary coordination sphere of the Eu^{3+} ion and neutralizing the charge on the cation. In the second possibility, one DGA arm of each of the two DGA ligands is participating in bonding, and the remaining inner-sphere coordination site of the cation is occupied by three nitrate ions, possibly via monodentate coordination. It is worth mentioning that the absence of water molecules in the first coordination sphere of Eu^{3+} was confirmed by fluorescence measurements (vide infra). The coordination of only one or two DGA units from each ligand can be rationalized in view of a large stereochemical impediment that may arise during the complexation.

One of the objectives of the present work was to investigate the effect of the spacer length on the extraction affinity of the ligands. The above-mentioned extraction data suggested that the stoichiometry of the extracted complexes was the same under identical experimental conditions. However, the absolute extraction values differed significantly for all the four ligands. Comparing the analogous ligands with C3 (L_I) and C2 (L_{II}) spacer atoms between the DGA moieties and the central N atom of the tripodal platform, the D_{Eu} value increases 14 times by one carbon atom difference (Table 1). As discussed above, if one assumes that only one DGA unit from both the ligands is participating in the bonding (in a stoichiometry of 1:2 metal/ligand complex), then a spacer atom may not have a significant effect on the complexation. However, in the case that one DGA arm from one ligand and two DGA arms from another ligand are complexing, then the spacer atom may impart a measurable effect. In such a case, increasing the spacer length will give more flexibility to the DGA arms attached to the central N atom and thereby may increase the extraction ability of the ligand. It needs to be mentioned here that in the case mentioned above, some of the amidic and etheric "O" atoms may not be coordinating to the metal ion. Our DFT studies did not indicate this (vide infra), and hence, the possibility of binding by two DGA arms from one ligand is ruled out. To get deep insight in this postulate, a detailed discussion is given in a later part of this article dealing with spectroscopic measurements and DFT calculations.

When we compare the effect of an alkyl group on the amidic nitrogen of the DGA units in the three analogous ligands L_{II} (R = H), L_{III} (R = Me), and L_{IV} (R = isopropyl), the D_{Eu} values follow the order: L_{III} > L_{IV} > L_{II} (Table 1). Ligand L_{III}, having a methyl group, yielded the best result having about 400 times higher D_{Eu} value than that obtained with L_{II}. Assumption of the +I effect on the coordinating >C═O group fails to explain the results, as the presence of an isopropyl group (L_{IV}) should give rise to better results. Earlier work[11b] on calix[4]arene functionalized DGA ligands revealed that the attachment of a suitable alkyl group on the amidic nitrogen of a DGA moiety helps in bringing the complexation sites to a favorable orientation by restricting the free rotation of the DGA arms. Such an effect may also be prevailing with the present ligands, but only if one assumes that one DGA unit from one ligand and two DGA units from another ligand are complexing. In this case, a methyl group appears to be the optimum as an isopropyl group may bring a stereochemical obstacle to the close DGA units resulting in a less favorable complexation.

Luminescence Spectroscopic Studies. To get more insight into the nature of the extracted complex, luminescence spectroscopic studies were carried out by extracting Eu^{3+} ion from 3 M HNO_3 by 1 mmol/L ligands. As shown in Figure 4a, the band features in the spectra originate from the

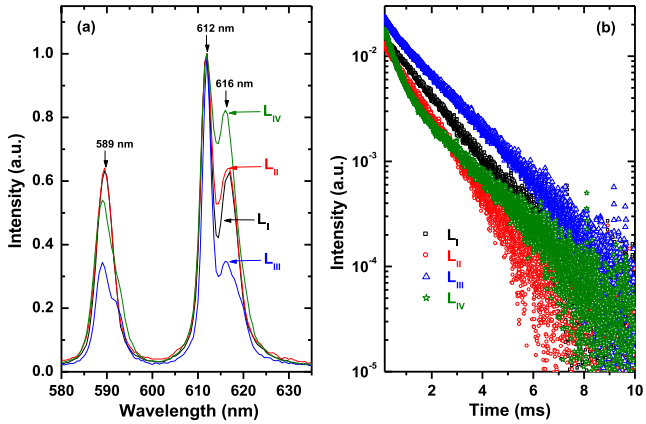

Figure 4. (a) Normalized emission spectra of Eu^{3+} in the extract. Organic phase: 1 mmol/L ligands in 5% isodecanol/*n*-dodecane; excitation: 394 nm. (b) Luminescence decay curve of the extracted Eu^{3+}. Excitation: 394 nm; Emission: 612 nm.

electronic transitions of the $^5D_0$ state to the $^7F_1$ (589 nm) and $^7F_2$ (612 nm) state of the Eu^{3+} ion.[18] The $^5D_0 \rightarrow {}^7F_2$ band (612 nm) is hypersensitive in nature, and its intensity increases upon complexation with the ligand due to replacement of water molecules from the coordination site of Eu^{3+}. On the other hand, the $^5D_0 \rightarrow {}^7F_1$ band (589) remains unaffected during the complexation. The ratio of the peak intensity (or band area) due to the $^5D_0 \rightarrow {}^7F_2$ and $^5D_0 \rightarrow {}^7F_1$ transition bands is referred to as the "asymmetry factor" and is generally used to understand the symmetry of the complex. As given in Table 2, the asymmetric factor for

Table 2. Lifetime and Asymmetric Factor (ratio of the areas of the 612 and 589 peaks) Data for the Eu^{3+} Ion in Different Complexes

complex	lifetime (μs)	$N_{H_2O(\pm 0.5)}$	asymmetric factor
$Eu(NO_3)_3(H_2O)_x$[a]	108	9.02	0.46
Eu^{3+}/L_I[b]	1461	0.02	0.68
Eu^{3+}/L_{II}[b]	1203	0.17	0.69
Eu^{3+}/L_{III}[b]	1753	0.00	0.71
Eu^{3+}/L_{IV}[b]	1650	0.00	0.71

[a]Data obtained in water. [b]Data obtained in a mixture of 95% *n*-dodecane containing 5% isodecanol.

DOI: 10.1021/acs.inorgchem.9b00985
Inorg. Chem. 2019, 58, 8633–8644

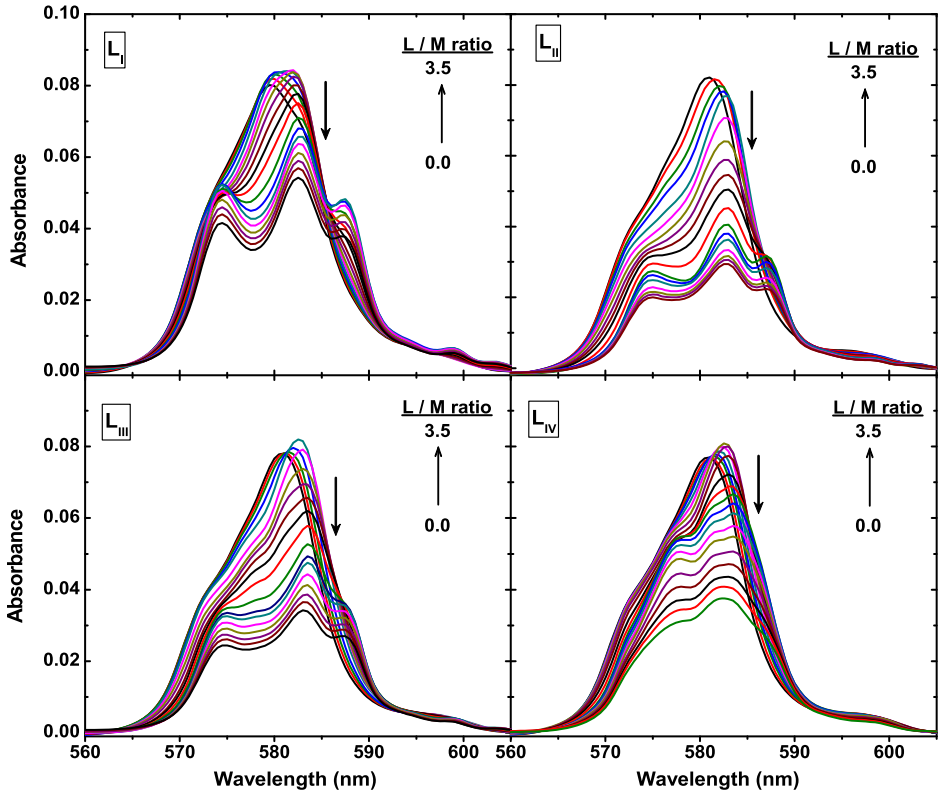

Figure 5. Spectrophotometric titration of Nd^{3+} with TREN-DGA in acetonitrile. L_I: cuvette: 4.5 mmol/L $Nd(NO_3)_3$ (2.0 mL); titrant: 25 mmol/L ligand in acetonitrile. The L/M ratio denotes the ligand to metal ratio. L/M refers to C_{Ligand}/C_{Nd} in the solution.

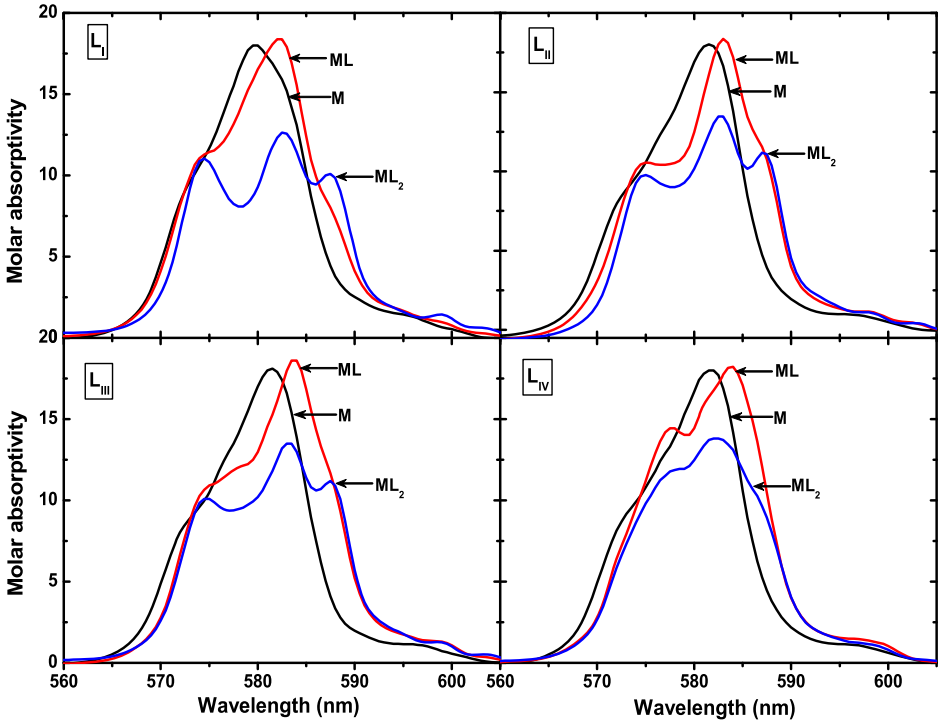

Figure 6. Deconvoluted spectra of Nd^{3+} (M), $Nd(L_{II})^{3+}$ (ML), and $Nd(L_{II})_2^{3+}$ (ML_2) species. Experimental conditions are the same as given for Figure 5.

the Eu^{3+}-aquo complex is 0.46, but it increased to around 0.7 upon complexation with all the four ligands. This feature indicates that the complexes that are extracted in the *n*-dodecane medium are not very distorted. On the other hand, a close observation of the 612 band, which is highly sensitive to the coordination environment around the Eu^{3+} atom, implies that the extracted complexes indeed differ in their nature. This band, which is a single band for the Eu^{3+}/aquo

DOI: 10.1021/acs.inorgchem.9b00985
Inorg. Chem. 2019, 58, 8633−8644

complex, splits into two giving a new emission band at 616 nm. Though our efforts to assign this new band were unsuccessful, it was clear that $\mathbf{L_I}$ and $\mathbf{L_{II}}$ formed very identical complexes as all their band intensities were similar. Splitting of the 612 nm band was more pronounced with $\mathbf{L_{IV}}$ due to the presence of the bulkier isopropyl group as compared with the other ligands, which may bring a larger asymmetry in the complex.

The number of water molecules present in the extracted complex, obtained from lifetime data (Figure 4b) using the standard Barthelemy − Choppin equation,[19]

$$N_{H_2O} = (1.05/\tau) - 0.7 \quad (4)$$

where τ is the lifetime in ms, indicated the absence of water molecules in the first coordination sphere of the Eu^{3+}/L complex. Addition of an inert nitrate salt, viz. tetramethylammonium nitrate, to the organic phase did not bring any change in the lifetime of the complexes, implying that the nitrate ions must have occupied a fixed position in the complex (inner sphere or outer sphere). As discussed earlier, if all the sites of the Eu^{3+} cation are occupied by the ligand, then the nitrate ions will remain in the outer sphere, merely neutralizing the charges. In contrast, if only six coordination sites (by two DGA moieties) are bonded with the ligands, then the nitrate will occupy the remaining sites in the inner sphere. However, there is no clear evidence from the fluorescence measurements about the actual position of the nitrate in the complex.

In order to substantiate the observations made in the extraction studies, we performed detailed complexation studies (in acetonitrile) using UV−vis spectrophotometry and luminescence spectroscopy. Acetonitrile was a judicious choice in the work as a single phase titration was not possible in *n*-dodecane due to the solubility issue of the metal ion (Eu^{3+}) in it. Additionally, acetonitrile is a poor coordinating ligand, similar to *n*-dodecane, and exhibits good solubility for the DGA ligands $\mathbf{L_I}$−$\mathbf{L_{IV}}$ as well as for the $Eu(NO_3)_3$/$Nd(NO_3)_3$ salts.

UV−visible Spectrophotometric Studies. In order to determine the complex formation constants, UV−vis spectrophotometric titrations were performed with Nd^{3+} in acetonitrile with $\mathbf{L_I}$−$\mathbf{L_{IV}}$. In these experiments, the hypersensitive transitions ($^4I_{9/2} \rightarrow {}^4G_{5/2}$, $^2G_{7/2}$) of Nd^{3+} in the visible wavelength region (550−610 nm)[20] were monitored as a function of the ligand concentration.

As shown in Figure 5, two absorbing complexes appeared upon progressive addition of ligand to the Nd^{3+} solution. Similar to luminescence spectral data (vide supra), the titration data could be best fit into three absorbing species, viz. free Nd^{3+}, $Nd{\cdot}(\mathbf{L_{II}})^{3+}$, and $Nd{\cdot}(\mathbf{L_{II}})_2{}^{3+}$. The deconvoluted spectra of the three species are shown in Figure 6, and their stability constants (log β) values are given in Table 3. The ESI-MS spectra were obtained for the Eu/$\mathbf{L_{III}}$ complex (as a representative ligand) and also confirmed the formation of a $Eu(\mathbf{L_{III}})^{3+}$ tripositive complex in acetonitrile as the limiting complex (Figure S1, Supporting Information).

An attempt was also made to determine the complex formation constants of the respective complexes with the Eu^{3+} ion with the four DGA ligands $\mathbf{L_I}$−$\mathbf{L_{IV}}$ by luminescence spectroscopy. The emission band of Eu^{3+} between 675−705 nm originates from the transitions of $^5D_0 \rightarrow {}^7F_4$, which is the electric dipole in nature and sensitive to the Eu^{3+} environment.[18] Any change in the coordination site of the Eu^{3+} shall bring a change in its spectral features due to its $^5D_0 \rightarrow {}^7F_4$ transitions. This feature of Eu^{3+} was used in the present work for the fluorescence titration with the ligands.

Table 3. Complexation Constant Data for Eu^{3+}/TREN-DGA Ligands in Acetonitrile at 25 °C

equilibrium reaction	method	log β
$Nd^{3+} + \mathbf{L_I} \rightarrow Nd(\mathbf{L_I})^{3+}$	UV−vis spectrophotometry	8.41
$Nd^{3+} + 2\mathbf{L_I} \rightarrow Nd(\mathbf{L_I})_2{}^{3+}$	UV−vis spectrophotometry	14.2
$Nd^{3+} + \mathbf{L_{II}} \rightarrow Nd(\mathbf{L_{II}})^{3+}$	UV−vis spectrophotometry	7.81
$Nd^{3+} + 2\mathbf{L_{II}} \rightarrow Nd(\mathbf{L_{II}})_2{}^{3+}$	UV−vis spectrophotometry	11.4
$Nd^{3+} + \mathbf{L_{III}} \rightarrow Nd(\mathbf{L_{III}})^{3+}$	UV−vis spectrophotometry	10.8
$Nd^{3+} + 2\mathbf{L_{III}} \rightarrow Nd(\mathbf{L_{III}})_2{}^{3+}$	UV−vis spectrophotometry	18.3
$Nd^{3+} + \mathbf{L_{IV}} \rightarrow Nd(\mathbf{L_{IV}})^{3+}$	UV−vis spectrophotometry	9.62
$Nd^{3+} + 2\mathbf{L_{IV}} \rightarrow Nd(\mathbf{L_{IV}})_2{}^{3+}$	UV−vis spectrophotometry	16.4
$Eu^{3+} + \mathbf{L_I} \rightarrow Eu(\mathbf{L_I})^{3+}$	luminescence	8.27
$Eu^{3+} + 2\mathbf{L_I} \rightarrow Eu(\mathbf{L_I})_2{}^{3+}$	luminescence	13.8
$Eu^{3+} + \mathbf{L_{II}} \rightarrow Eu(\mathbf{L_{II}})^{3+}$	luminescence	7.20
$Eu^{3+} + 2\mathbf{L_{II}} \rightarrow Eu(\mathbf{L_{II}})_2{}^{3+}$	luminescence	11.9
$Eu^{3+} + \mathbf{L_{III}} \rightarrow Eu(\mathbf{L_{III}})^{3+}$	luminescence	11.7
$Eu^{3+} + 2\mathbf{L_{III}} \rightarrow Eu(\mathbf{L_{III}})_2{}^{3+}$	luminescence	19.2
$Eu^{3+} + \mathbf{L_{IV}} \rightarrow Eu(\mathbf{L_{IV}})^{3+}$	luminescence	10.1
$Eu^{3+} + 2\mathbf{L_{IV}} \rightarrow Eu(\mathbf{L_{IV}})_2{}^{3+}$	luminescence	16.9

As shown in Figure 7, when ligand was added into the Eu^{3+} solution, the $^5D_0 \rightarrow {}^7F_4$ band (685 nm) was significantly sensitized, and finally a new emission band at 695 nm became prominent. Though the degree of sensitization was different for the four ligands, all the ligands gave a common emission band at 695 nm for the ultimate complex. For all the ligands, changes in the spectral features were observed up to a ligand/metal (L/M) ratio of about 2.0, beyond which only dilution of the complex was observed, indicating the formation of limiting Eu^{3+}/L complexes. The titration data of all the four ligands could be best fitted into the two emitting complexes $(Eu{\cdot}L)^{3+}$ and $(Eu{\cdot}L_2)^{3+}$, and their stability constants (log β) are also given in Table 3. The stability constant values followed an order identical to that observed with the distribution measurements, viz., $\mathbf{L_{III}} > \mathbf{L_{IV}} > \mathbf{L_I} > \mathbf{L_{II}}$. Interestingly, the log β values obtained from the luminescence data are in close agreement with those obtained with UV−vis spectrophotometry (taking into consideration slight difference due to two different lanthanide ions). This study also suggests that though luminescence data are not generally used for log β determination, it can be considered if the 695 emission band is used instead of the 615 band.

We could not perform the titration in the entire range as the emission due to the $^5D_0 \rightarrow {}^7F_2$ transition (612 nm) was giving a very high quantum yield, and under such conditions, the band due to the $^5D_0 \rightarrow {}^7F_4$ transition (695 nm) was difficult to record due to its poor quantum yield and instrument limitations. On the basis of the spectra shown in Figure 8a, the "asymmetry factor" values were calculated; they are given in Table 4. The lifetime data (Figure 8b) confirmed that no water occupies the primary hydration sphere of Eu in all the four complexes.

DFT Studies. *Structural Parameters.* The minimum energy structures of the free DGA ligands $\mathbf{L_I}$−$\mathbf{L_{IV}}$ are given in the Supporting Information (Figure S2), while those of their complexes with Eu^{3+}, in the absence and presence of nitrate are displayed in Figure 9. The calculated structural parameters for the Eu^{3+} complexes, in the absence and presence of nitrate, are presented in Table 5. The metal

DOI: 10.1021/acs.inorgchem.9b00985
Inorg. Chem. 2019, 58, 8633−8644

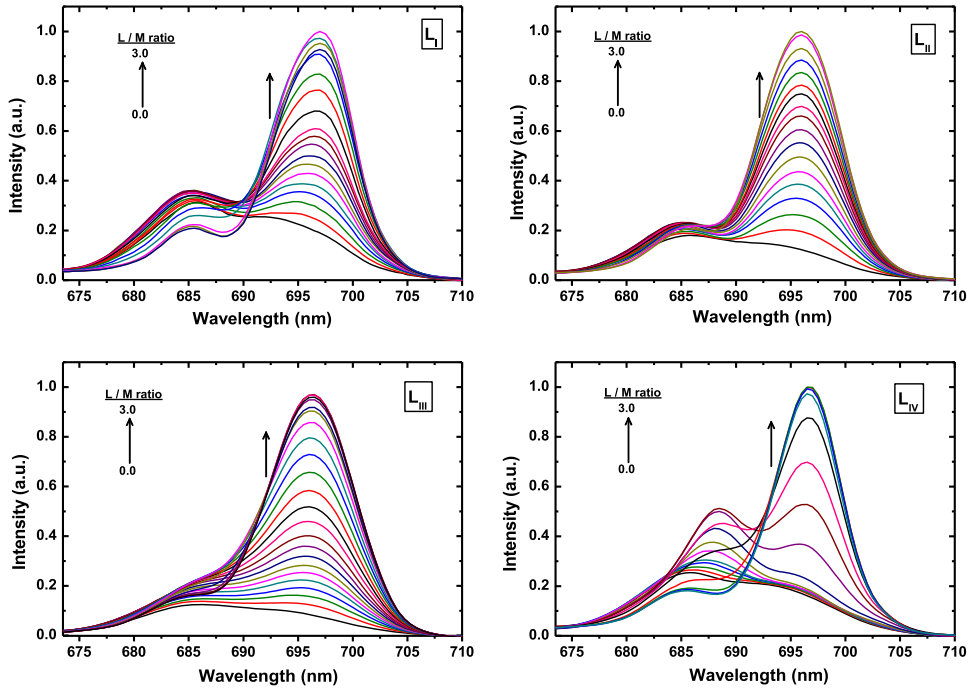

Figure 7. Fluorescence titration of Eu(III) with DGA ligands $\mathbf{L_{I-IV}}$ in acetonitrile. Cuvette: 0.12 mmol/L $Eu(NO_3)_3$ (1.5 mL); titrant: 1.0 mmol/L ligand in acetonitrile. L/M ratio denotes the ligand to metal ratio.

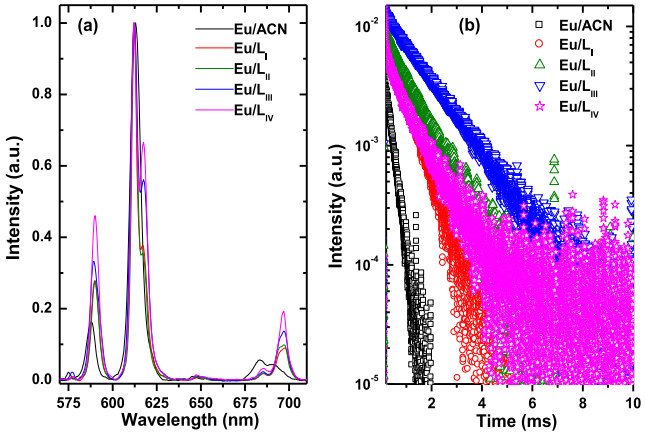

Figure 8. Normalized emission spectra (a), and luminescence decay curves (b) of $Eu^{3+}/\mathbf{L_{I-IV}}$ final complexes in acetonitrile. Experimental conditions are the same as those given in Figure 4. Excitation: 394 nm; emission: 612 nm.

Table 4. Lifetime and Asymmetric Factor Data for the Eu^{3+} Ion in Different Complexes

complex	lifetime (μs)	$N_{H_2O(\pm 0.5)}$	asymmetric factor
$Eu(NO_3)_3$ [a]	108	9.02	0.46
$Eu(NO_3)_3$ [b]	228	3.91	7.09
Eu^{3+}/L_I [b]	990	0.36	4.07
Eu^{3+}/L_{II} [b]	1011	0.34	3.97
Eu^{3+}/L_{III} [b]	1430	0.03	3.68
Eu^{3+}/L_{IV} [b]	1273	0.12	3.14

[a]Data obtained in water. [b]Data obtained in acetonitrile.

oxygen bond distances with the amidic O atoms were found to be shorter than those of the etheric O atoms, indicating that the former leads to stronger interactions than the latter. However, in the presence of a nitrate ion, the metal oxygen bond distances with the nitrate O atoms were found to be shorter than those of the both amidic O and ethereal O atoms. Our previous report[13a] using DFT and extended X-ray absorption fine structure (EXAFS) studies also indicated participation of one of the DGA arms from each of the two tripodal DGA ligands where four amidic and two etheric "O" atoms were suggested to coordinate to the Eu^{3+} ion apart from the three monodentate nitrate ions. Similar geometries are proposed for the present set of ligands.

Thermodynamic Free Energy of Complexation. The free energy for the complexation of Eu^{3+} ion with DGA ligands $\mathbf{L_I}$–$\mathbf{L_{IV}}$ in acetonitrile is presented in Table 6. The explicit hydration of Eu^{3+} ion with nine water molecules in the first solvation shell was considered for evaluating the complexation free energy as it was found to reproduce the experimental solvation energy quite accurately.[21] The entropy of complexation was found to be positive and quite high as per calculations given in the Supporting Information. The well-known COSMO solvation approach was used to simulate the solvent phase as it was able to predict properties quite accurately. The acetonitrile organic phase was modeled using a dielectric constant of 37.5. The calculated solution phase free energies of binding are given in Table 6 and follow the trend in. In the absence of nitrate ions as $\mathbf{L_{III}} > \mathbf{L_I} > \mathbf{L_{II}} > \mathbf{L_{IV}}$, and those in the presence of nitrate ions as $\mathbf{L_{III}} > \mathbf{L_{IV}} > \mathbf{L_{II}} > \mathbf{L_I}$.

Bonding Analysis. In order to get insight into the nature of the bonding in the complexes of Eu^{3+} ions with DGA ligands $\mathbf{L_I}$–$\mathbf{L_{IV}}$, the charge on the metal ion and the atomic orbital population in the complexes were analyzed using the method of natural population analysis (NPA).[22] The calculated values are presented in Table S1. The substantial positive charge on the Eu^{3+} ion indicates an ion-dipole type of interaction in all cases. From NPA, it is revealed that there is a small extra orbital contribution to the inner s, and f subshells and a significant contribution in the d subshells of the metal ion,

DOI: 10.1021/acs.inorgchem.9b00985
Inorg. Chem. 2019, 58, 8633–8644

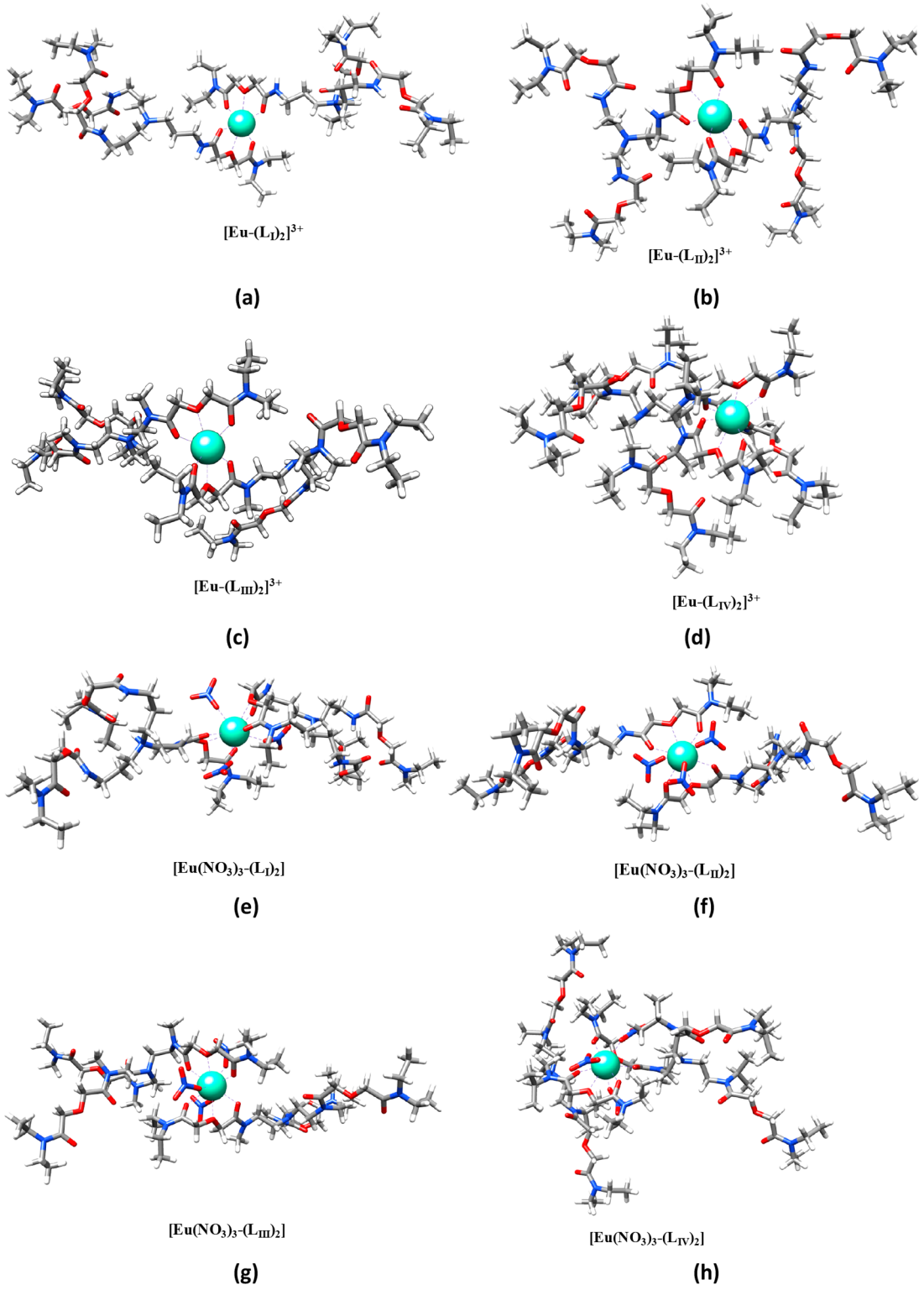

Figure 9. Optimized structures of complexes of $\mathbf{L_I}$−$\mathbf{L_{IV}}$ with Eu^{3+} in the absence (a−d) and presence of nitrate ions (e−h) at the B3LYP/SVP level of theory.

indicating that the interaction of Eu^{3+} with a ligand has some covalent character. The d subshells were found to be more diffused than the s and f subshells. In order to understand the nature of the interaction, the energy gap of the E_{HOMO} and E_{LUMO} for the free metal ion and the ligands $\mathbf{L_I}$−$\mathbf{L_{IV}}$ was evaluated and is listed in Table S2. The ligands $\mathbf{L_I}$−$\mathbf{L_{IV}}$, having hard O donor atoms, belong to the class of hard bases as evident from the high $E_{HOMO-LUMO}$, χ (absolute electronegativity) and η (absolute hardness) values. As per the HSAB principle, the closer the value of $E_{HOMO-LUMO}$ for the donor and acceptor the higher will be the interaction energy. Here, the $E_{HOMO-LUMO}$ of the Eu^{3+} ion (5.20 eV) is very close to the values of $\mathbf{L_I}$−$\mathbf{L_{IV}}$ (5.80−5.88 eV). The calculated values of the absolute electronegativity η and the absolute electronegativity

DOI: 10.1021/acs.inorgchem.9b00985
Inorg. Chem. 2019, 58, 8633−8644

Table 5. Calculated Structural Parameters of the Complexes of Eu^{3+} with DGA Ligands L_I–L_{IV} in the Absence as well as Presence of Nitrate Ions at the B3LYP Level of Theory Using the SVP Basis Set

system	Eu–$O_{C=O}$ (Å)	Eu–$O_{ethereal}$ (Å)	Eu–O_{NO_3} (Å)
$Eu(L_I)_2^{3+}$	2.515, 2.428, 2.445, 2.449	2.687, 2.673	
$Eu(L_{II})_2^{3+}$	2.384, 2.388, 2.402, 2.404	2.601, 2.652	
$Eu(L_{III})_2^{3+}$	2.407, 2.506, 2.427, 2.398	2.672, 2.678	
$Eu(L_{IV})_2^{3+}$	2.451, 2.495, 2.368, 2.420	2.513, 2.748	
$Eu(NO_3)_3(L_I)_2$	2.473, 2.483, 2.515, 2.549	2.760, 2.765	2.390, 2.508, 2.509
$Eu(NO_3)_3(L_{II})_2$	2.424, 2.479, 2.482, 2.560	2.627, 2.638	2.277, 2.387, 2.431
$Eu(NO_3)_3(L_{III})_2$	2.403, 2.414, 2.505, 2.511	2.646, 2.728	2.337, 2.394, 2.403
$Eu(NO_3)_3(L_{IV})_2$	2.411, 2.425, 2.438, 2.458	2.644, 2.713	2.333, 2.434, 2.445

Table 6. Calculated Values of the Gibbs Free Energy (kcal/mol) of Binding of Different Eu^{3+} Complexes of DGA Ligands L_I–L_{IV} in Acetonitrile at the B3LYP/TZVP Level of Theory

equilibrium reaction	free energy of complexation (kcal/mol)
$Eu^{3+} + 2L_I \rightarrow Eu(L_I)_2^{3+}$	−36.7
$Eu^{3+} + 2L_{II} \rightarrow Eu(L_{II})_2^{3+}$	−34.8
$Eu^{3+} + 2L_{III} \rightarrow Eu(L_{III})_2^{3+}$	−36.8
$Eu^{3+} + 2L_{IV} \rightarrow Eu(L_{IV})_2^{3+}$	−33.9
$Eu^{3+} + 3NO_3^- + 2L_I \rightarrow Eu(L_I)_2^{3+}$	17.61
$Eu^{3+} + 3NO_3^- + 2L_{II} \rightarrow Eu(L_{II})_2^{3+}$	−12.14
$Eu^{3+} + 3NO_3^- + 2L_{III} \rightarrow Eu(L_{III})_2^{3+}$	−24.59
$Eu^{3+} + 3NO_3^- + 2L_{IV} \rightarrow Eu(L_{IV})_2^{3+}$	−19.16

χ were found to be very close for these ligands. The binding energy trend cannot be correlated with the values of η and χ. The amount of charge transfer ΔN was also evaluated for the donor–acceptor interaction; the values are presented in Table S2. The higher the value of ΔN, the higher is the metal–ligand interaction. In the present case, the value of ΔN was found to be very close for all the studied ligands, and hence a correlation with the binding energy could not be made.

CONCLUSIONS

N-Pivot tripodal DGA ligands L_I–L_{IV} form 1:2 M:L complexes as evident from solvent extraction and confirmed by luminescence spectroscopic studies. This is in sharp contrast to the 1:3 (M:L) complexes reported for the extraction of trivalent rare earth (and actinide) ions with TODGA. Furthermore, the participation of only two DGA arms from each of the tripodal DGA ligands in the present study can be attributed to possible steric constraints experienced with these preorganized ligands, which was not the case with TODGA. However, in spite of this, the extracted complexes were assumed to be highly lypophilic (probably due to no coordinated water in the inner-sphere) and resulted in enormously high distribution ratio values at millimolar concentrations. Luminescence studies also indicated complete dehydration of the inner-coordination sphere during complexation, which was also confirmed by the large complex formation constants. Introduction of electron-donating alkyl groups on the amidic nitrogen atom of the DGA and enlargement of the spacer between the pivotal N atom and the DGA unit positively influence the complexation ability, as compared with the previously described TREN-DGA (ligand L_{II}). Though the mode of complexation including the role of nitrate ions as inner- or outer-sphere coordination was not clearly understood from the spectroscopic studies, DFT computations suggested participation of nitrate ions in the inner-sphere (most probably in a monodentate manner), which would indicate the participation of only one DGA arm from each of the N-pivot ligands L_I–L_{IV}. This study clearly demonstrates that subtle changes in the ligand design may give rise to improved complexation properties. The results are quite interesting, and these relatively simple ligands may be used for the separation of actinide ions from radioactive feed solutions.

EXPERIMENTAL SECTION

General. Tris(2-(*N*-methyl)aminoethyl)amine (Me_3TREN), tris-(2-(*N*-isopropyl)aminoethyl)amine (iPr_3TREN), tris(2-aminopropyl)amine (TRPN), triethylamine (Et_3N), *n*-dodecane, isodecanol, acetonitrile, and AmberlystA21 were procured from Sigma-Aldrich in their highest available purity. 4-Nitrophenyl 2-(2-(dioctylamino)-2-oxoethoxy)acetate was synthesized according to a reported procedure.[23] Stock solutions of Eu^{3+} and Nd^{3+} ions were prepared by dissolving $Eu(NO_3)_3{\cdot}5H_2O$ and $Nd(NO_3)_3{\cdot}6H_2O$ (Sigma-Aldrich), respectively, in acetonitrile and subsequently standardized by EDTA complexometric titration using methylthymol blue as the indicator.[24] Whereas ^{241}Am radiotracer was used from the laboratory stock, ^{152,154}Eu was obtained from BRIT, Mumbai. The purity of radiotracers was confirmed prior to their use by alpha and gamma spectrometry. All the other reagents were of AR grade and were used without further purification.

^{1}H and ^{13}C NMR spectra were recorded on a Bruker 400 MHz NMR spectrometer. ESI mass spectra were recorded on a Micromas LCT ESI-TOF mass spectrometer with LCT V4.1 SCN728 software from Waters, Inc.

General Procedure for the Preparation of Ligands L_I–L_{IV}. A solution of 4-nitrophenyl 2-(2-(dioctylamino)-2-oxoethoxy)acetate (1.02 equiv per amino group), triamine (0.5 mmol, 1 equiv) and triethylamine (1.03 equiv. per amino group) in dry toluene (15 mL) was refluxed for 15 h. A chromatography glass column (2 cm Ø) was loaded with Amberlyst A21 (20 g) suspended in MeOH (30 mL). The resin was washed with MeOH (70 mL) and Et_2O (100 mL), at the end keeping solvent above the resin, whereupon a pluck of cotton was placed. After removal of the toluene, the residue of the reaction was dissolved in Et_2O (15 mL) and loaded slowly on top of the wet resin inside the column. The solution was slowly eluted through the column with Et_2O (185 mL). The solvent was evaporated to yield the products as an oil. In the ^{1}H NMR spectra, only one-third of the number of hydrogen atoms is given, since the ligands are symmetrical.

Ligand L_I was prepared using 4-nitrophenyl 2-(2-(dioctylamino)-2-oxoethoxy)acetate (730 mg, 1.53 mmol), TRPN (94 mg, 0.5 mmol), and Et_3N (157 mg, 1.55 mmol) in dry toluene (15 mL). It was obtained as a colorless oil in 64% yield.

^{1}H NMR (400 MHz, $CDCl_3$) δ = 7.80 (t, J = 5.6 Hz, 1H), 4.22 (s, 2H), 4.03 (s, 2H), 3.33–3.24 (m, 4H), 3.08 (t, J = 8.0 Hz, 2H), 2.42 (t, J = 6.9 Hz, 2H), 1.64 (t, J = 6.9 Hz, 2H), 1.55–1.46 (m, 4H), 1.32–1.20 (m, 20H), 0.86 (t, J = 6.8 Hz, 3H), 0.85 (t, J = 6.8 Hz, 3H). ^{13}C NMR (101 MHz, $CDCl_3$) δ = 169.4, 168.1, 71.7, 69.5, 51.6, 46.8, 46.1, 37.4, 31.8, 31.7, 29.4, 29.31, 29.28, 29.23, 29.19, 29.0, 27.6, 27.0, 26.9, 26.8, 22.7, 22.6, 14.1, 14.0. ESI-MS: m/z 1207.0 $[M + H]^+$; HRMS: m/z calcd for $C_{69}H_{136}N_7NaO_9$: 615.0143 $[M + H + Na]^{2+}$; found 615.0111.

Ligand L_{II}. For the details of the synthesis and the spectral data see ref 13a.

DOI: 10.1021/acs.inorgchem.9b00985
Inorg. Chem. 2019, 58, 8633–8644

Ligand L_{III} was prepared using 4-nitrophenyl 2-(2-(dioctylamino)-2-oxoethoxy)acetate (730 mg, 1.53 mmol), Me_3TREN (95 mg, 0.5 mmol), and Et_3N (157 mg, 1.55 mmol) in dry toluene (15 mL). It was obtained as a colorless oil in 76% yield.

^{1}H NMR (400 MHz, $CDCl_3$) δ = 4.35−4.25 (m, 4H), 3.43−3.36 (m, 2H), 3.31−3.24 (m, 2H), 3.20−3.10 (m, 2H), 2.99 (d, J = 2.0 Hz, 2H), 2.95 (d, J = 2.0 Hz, 1H), 2.75−2.62 (m, 2H), 1.56−1.45 (m, 4H), 1.33−1.20 (m, 20H), 0.87 (t, J = 6.9 Hz, 3H), 0.86 (t, J = 6.9 Hz, 3H). ^{13}C NMR (101 MHz, $CDCl_3$) δ = 168.8, 168.4, 69.4, 69.1, 52.6, 51.4, 51.2, 47.9, 46.9, 46.2, 46.1, 45.8, 35.0, 34.96, 33.92, 31.80, 31.75, 29.40, 29.37, 29.32, 29.25, 29.2, 29.0, 27.6, 27.1, 26.9, 22.7, 22.6, 14.1. ESI-MS: m/z 1207.0 $[M + H]^+$; HRMS: m/z calcd for $C_{69}H_{136}N_7O_9$: 1207.0394 $[M + H]^+$; found 1207.0372.

Ligand L_{IV} was prepared using 4-nitrophenyl 2-(2-(dioctylamino)-2-oxoethoxy)acetate (730 mg, 1.53 mmol), iPr_3TREN (136 mg, 0.5 mmol), and Et_3N (157 mg, 1.55 mmol) in dry toluene (15 mL). It was obtained as a colorless oil in 92% yield.

^{1}H NMR (400 MHz, $CDCl_3$) δ = 4.52 (hept, J = 6.3 Hz, 0.25H) 4.38−4.20 (m, 4H), 3.97 (hept, J = 6.3 Hz, 0.75H), 3.33−3.22 (m, 4H), 3.19−3.11 (m, 2H), 2.76−2.62 (m, 2H), 1.56−1.45 (m, 4H), 1.33−1.21 (m, 20H), 1.21−1.16 (m, 6H), 0.87 (t, J = 6.9 Hz, 3H), 0.86 (t, J = 6.9 Hz, 3H). ^{13}C NMR (101 MHz, $CDCl_3$) δ = 168.4, 168.2, 69.9, 69.2, 53.0, 47.5, 46.9, 45.8, 39.5, 31.8, 31.7, 29.4, 29.31, 29.25, 29.2, 28.9, 27.6, 27.1, 26.8, 22.7, 22.6, 21.4, 21.3, 20.4, 14.1. ESI-MS: m/z 1291.1 $[M + H]^+$; HRMS: m/z calcd for $C_{75}H_{148}N_7O_9$: 1291.1333 $[M + H]^+$; found 1291.1364.

Distribution Measurements. Ligand solutions (1 mmol/L) for solvent extraction experiments were prepared by dissolving the known weight of ligands in 5% isodecanol/n-dodecane. The distribution ratios of Am^{3+} and Eu^{3+} were measured by equilibrating 1 mL of the ligand solution with an equal volume of the aqueous phase of desired acidity spiked with the required radiotracer. The equilibration was carried out in a stoppered Pyrex glass tube of 10 mL capacity at 25 ± 0.1 °C. Sufficient equilibration time (2 h) was given for reaching the equilibrium,[13b] whereupon the tubes were centrifuged. Suitable volumes of the organic and aqueous phases were removed for assaying by gamma counting using a well type NaI(Tl) scintillation counter. The concentrations of Am and Eu in the radiotracer studies were 10^{-7} M and 10^{-5} M, respectively. Distribution coefficients (D) were calculated as the ratio of the counts of the radionuclides in the ligand phase to that in an equal volume of the aqueous phase. All the experiments were carried out in triplicate, and the accepted data were within the limit of a relative standard deviation of ±5%.

Luminescence Measurements. Luminescence emission spectra and the lifetimes of Eu^{3+} were recorded on a PTI QuantaMaster 400 instrument. The signals were recorded and analyzed using PTI FelixGX software from the PTI QuantaMaster. The emission spectra of Eu^{3+} extracted in the n-dodecane phase were recorded in the wavelength region of 600−630 nm (hypersensitive transitions of $^5D_0 \rightarrow {}^7F_2$) by excitation at 394 nm. The emission lifetime data were recorded in the time-resolved mode by excitation at 394 nm and following the decay of the 612 nm emission band.

Fluorescence titration on Eu^{3+}/ligand complexation was performed in acetonitrile by recording the emission spectra in the region 670−710 nm ($^5D_0 \rightarrow {}^7F_4$ transition) by excitation at 394 nm. Titrations were performed in acetonitrile, as single phase titration was not possible in n-dodecane due to the solubility issue of Eu^{3+} in this paraffinic solvent. Use of acetonitrile was a judicious choice due to its poor coordinating nature, and free solubility of ligand and $Eu(NO_3)_3$ in it. A solution of Eu^{3+} was kept in a 4 mL cuvette and titrated with standard ligand solutions. Emission spectra were recorded after adding an appropriate aliquot of ligand into the cuvette and mixing thoroughly for about 2 min. The mixing time was found to be sufficient to complete the complexation. For each set of titration, usually 30−35 spectra were recorded. The stability constants of the Eu^{3+}/L complexes, where L = DGA ligands L_I−L_{IV}, were calculated by nonlinear least-squares regression analysis using the HyperSpec program,[25] based on the following equilibrium reaction:

$$Eu^{3+} + iL \rightleftharpoons Eu(L_i)^{3+} \quad (5)$$

$$\beta_i = [Eu(L_i)^{3+}]/[Eu^{3+}][L]^i \quad (6)$$

where β_i is the overall complex formation constant of the i^{th} complex.

UV−vis Absorption Spectroscopy. Spectrophotometric titrations were performed with Nd^{3+} in acetonitrile. The hypersensitive transitions ($^4I_{9/2} \rightarrow {}^4G_{5/2}$, $^2G_{7/2}$) of Nd^{3+} in the visible wavelength region (550−610 nm)[20] were monitored as a function of ligand concentration. The spectrophotometric titration was performed on a double beam Jasco V-530 spectrophotometer using 10 mm path length Quartz cells. The initial concentration of Nd^{3+} in the cell was ∼8 mmol/L, and the titrant was ∼25 mmol/L ligand in acetonitrile. Similar to the fluorescence titration, 25−30 titrations points were recorded, and the stability constants of the Nd^{3+}/L complexes were calculated using the HypSpec program.[25]

DFT Calculations. Structures of the free DGA ligands L_I−L_{IV} and its complexes with Eu^{3+} ion in the absence and presence of nitrate ion were optimized using the Becke-Lee-Young-Parr (B3LYP) density functional[26] employing the split-valence plus polarization (SVP) basis set[27] as implemented in the TURBOMOLE suite of program.[28] The scalar relativistic effective core potentials (ECP) were used for the Eu^{3+} ion where 28 electrons were kept in the core for Eu.[29] The septate spin state was used during the computation of structure and energy. Optimization was performed without any symmetry restrictions. The free energy was computed at 298.15 K using the B3LYP functional.[26] The hybrid B3LYP functional was shown to be quite successful in predicting the thermodynamic properties of actinides.[30] The solvent phase was accounted for using the popular conductor like screening model (COSMO).[31] The dielectric constant of acetonitrile was taken to be 37.5. The model complexation reaction was used as follows:

$$Eu^{3+}{}_{(org)} + 3NO_3^-{}_{(org)} + 2L_{(org)} \rightarrow Eu(NO_3)_3(L)_{2(org)} \quad (7)$$

The free energy of extraction, ΔG_{ext}, for the above complexation reaction was evaluated using our earlier reported thermodynamic procedure.[32]

Scalar relativistic effects for the heavier lanthanide and actinide elements were included in the present computation using an earlier reported procedure.[33] Since there is a very small effect on the solvation energy between the gas phase and the solvent phase geometry,[34] the aqueous solvent effect was integrated by performing single point energy calculations using the optimized geometry obtained from the B3LYP level of theory employing the COSMO solvation model.

■ ASSOCIATED CONTENT

Supporting Information

The Supporting Information is available free of charge on the ACS Publications website at DOI: 10.1021/acs.inorgchem.9b00985.

Purification and assay radioisotopes, DFT data, coordinates ligand (complexes) (PDF)

■ AUTHOR INFORMATION

Corresponding Authors

*E-mail: mpatra@barc.gov.in (P.K.M.).
*E-mail: w.verboom@utwente.nl (W.V.).

ORCID

Seraj A. Ansari: 0000-0002-2242-6876
Prasanta K. Mohapatra: 0000-0002-0577-1811
Sk. Musharaf Ali: 0000-0003-0457-0580
Jurriaan Huskens: 0000-0002-4596-9179
Willem Verboom: 0000-0002-6874-3842

DOI: 10.1021/acs.inorgchem.9b00985
Inorg. Chem. 2019, 58, 8633−8644

Notes

The authors declare no competing financial interest.

■ ACKNOWLEDGMENTS

Some of the authors (S.A.A., P.K.M.) wish to thank Dr. P. K. Pujari, Head, Radiochemistry Division, Bhabha Atomic Research Centre, for his keen interest. S.M.A. wishes to thank Mr. K. T. Shenoy for his constant encouragement. The authors gratefully acknowledge the help rendered by Dr. P. K. Verma during the luminescence measurements and that by Dr. Pranaw Kumar for ESI-MS analysis.

■ REFERENCES

(1) (a) Ansari, S. A.; Pathak, P. N.; Mohapatra, P. K.; Manchanda, V. K. Chemistry of Diglycolamides: Promising Extractants for Actinide Partitioning. *Chem. Rev.* **2012**, *112*, 1751−1772. (b) Whittaker, D.; Geist, A.; Modolo, G.; Taylor, R.; Sarsfield, M.; Wilden, A. Applications of Diglycolamide Based Solvent Extraction Processes in Spent Nuclear Fuel Reprocessing, Part 1: TODGA. *Solvent Extr. Ion Exch.* **2018**, *36*, 223−256.

(2) (a) *Nuclear Energy Research and Development Roadmap: Future Pathways*; BIS/13/632, HM Gov., 2013 (b) Salvatores, M. Nuclear fuel cycle strategies including partitioning and transmutation. *Nucl. Eng. Des.* **2005**, *235*, 805−816. (c) Modolo, G.; Geist, A.; Miguirditchian, M. Minor actinide separations in the reprocessing of spent nuclear fuels: Recent advances in Europe. In *Reprocessing and Recycling of Spent Nuclear Fuel*; Taylor, R. J., Ed.; Woodhead Publishing: Oxford, UK, Chapter 10, 2015; pp 246−287. (d) Ramana, M. V. Technical and social problems of nuclear waste. In *Wiley Interdisciplinary Reviews: Energy and Environment* **2018**, *7*, E289.

(3) (a) Horwitz, E. P.; Kalina, D. G.; Diamond, H.; Vandegrift, G. H.; Schulz, W. W. The TRUEX process: A process for the extraction of trans-uranium elements from nitric acid wastes using modified PUREX solvent. *Solvent Extr. Ion Exch.* **1985**, *3*, 75−109. (b) Veliscek-Carolan, J. Separation of actinides from spent nuclear fuel: A review. *J. Hazard. Mater.* **2016**, *318*, 266−281. (c) Ansari, S. A.; Pathak, P. N.; Mohapatra, P. K.; Manchanda, V. K. Aqueous partitioning of minor actinides by different processes. *Sep. Purif. Rev.* **2011**, *40*, 43−76.

(4) (a) Nash, K. L.; Madic, C.; Mathur, J. N.; Lacquement, J. Actinide separation and technology. In *The Chemistry of the Actinide and Transactinide Elements*, 3rd ed.; Morss, L. R., Edelstein, N. M., Fuger, J.; Katz, J. J., Eds.; Springer, 2006; Vol. *4*, p. 2622. (b) Madic, C.; Hudson, M. J.; Liljenzin, J. O.; Glatz, J.-P.; Nannicini, R.; Facchini, A.; Kolarik, Z.; Odoj, Z. R. *New Partitioning Techniques for Minor Actinides*; EUR 19149; European Commission: Luxembourg, 2000. (c) Leoncini, A.; Huskens, J.; Verboom, W. Ligands for f-element extraction used in the nuclear fuel cycle. *Chem. Soc. Rev.* **2017**, *46*, 7229−7273.

(5) (a) Jensen, M. P.; Yaita, T.; Chiarizia, R. Reverse-Micelle Formation in the Partitioning of Trivalent f-Element Cations by Biphasic Systems Containing a Tetraalkyldiglycolamide. *Langmuir* **2007**, *23*, 4765−4774. (b) Yaita, T.; Herlinger, A. W.; Thiyagarajan, P.; Jensen, M. P. Influence of Extractant Aggregation on the Extraction of Trivalent f-Element Cations by a Tetraalkyldiglycolamide. *Solvent Extr. Ion Exch.* **2004**, *22*, 553−571. (c) Nave, S.; Modolo, G.; Madic, C.; Testard, F. Aggregation Properties of *N,N,N′,N′*-Tetraoctyl-3- oxapentanediamide (TODGA) in n-Dodecane. *Solvent Extr. Ion Exch.* **2004**, *22*, 527−551. (d) Pathak, P. N.; Ansari, S. A.; Kumar, S.; Tomar, B. S.; Manchanda, V. K. Dynamic light scattering study on the aggregation behaviour of N,N,N′,N′-tetraoctyl diglycolamide (TODGA) and its correlation with the extraction behaviour of metal ions. *J. Colloid Interface Sci.* **2010**, *342*, 114−118. (e) Ganguly, R.; Sharma, J. N.; Choudhury, N. Phase separation in the TODGA reverse micellar solutions in dodecane: identifying an upper consolute temperature and an associated critical behaviour. *Soft Matter* **2012**, *8*, 1795−1800.

(6) (a) Tian, G.; Shuh, D. K.; Beavers, C. M.; Teat, S. J. A structural and spectrophotometric study on the complexation of Am(III) with TMOGA in comparison with the extracted complex of DMDOOGA. *Dalton Trans.* **2015**, *44*, 18469−18474. (b) Kou, F.; Yang, S.; Qian, H.; Zhang, L.; Beavers, C. M.; Teat, S. J.; Tian, G. A fluorescence study on the complexation of Sm(iii), Eu(iii) and Tb(iii) with tetraalkyldiglycolamides (TRDGA) in aqueous solution, in solid state, and in solvent extraction. *Dalton Trans.* **2016**, *45*, 18484−18493. (c) Wilden, A.; Modolo, G.; Lange, S.; Sadowski, F.; Beele, B. B.; Skerencak-Frech, A. S.; Panak, P. J.; Iqbal, M.; Verboom, W.; Geist, A.; Bosbach, D. Modified diglycolamides for the An(III) + Ln(III) co-separation: Evaluation by solvent extraction and time-resolved laser fl uorescence spectroscopy. *Solvent Extr. Ion Exch.* **2014**, *32*, 119−137.

(7) Tian, G.; Teat, S. J.; Rao, L. Structural and Thermodynamic Study of the Complexes of Nd(III) with N,N,N′,N′-Tetramethyl-3-oxa-glutaramide and the Acid Analogues. *Inorg. Chem.* **2014**, *53*, 9477−9485.

(8) (a) Narita, H.; Yaita, T.; Tachimori, S. *Proceedings of International Solvent Extraction Conference*, 1999 (ISEC99), pp 693−696. (b) Antonio, M. R.; McAlister, D. R.; Horwitz, E. P. An europium(III) diglycolamide complGex: insights into the coordination chemistry of lanthanides in solvent extraction. *Dalton Trans.* **2015**, *44*, 515−521.

(9) Sasaki, Y.; Zhu, Z.-X.; Sugo, Y.; Kimura, T. Extraction of various metal ions from nitric acid to n-dodecane by diglycolamide (DGA) compounds. *J. Nucl. Sci. Technol.* **2007**, *44*, 405−409.

(10) (a) Matloka, K.; Gelis, A.; Regalbuto, M.; Vandegrift, G.; Scott, M. J. C3-Symmetric Tripodal Thio/Diglycolamide-Based Ligands for Trivalent f-Element Separations. *Sep. Sci. Technol.* **2006**, *41*, 2129−2146. (b) Matloka, K.; Gelis, A.; Regalbuto, M.; Vandegrift, G.; Scott, M. J. Highly efficient binding of trivalent f-elements from acidic media with a C3-symmetric tripodal ligand containing diglycolamide arms. *Dalton Trans.* **2005**, 3719−3721. (c) Jańczewski, D.; Reinhoudt, D. N.; Verboom, W.; Hill, C.; Allignol, C.; Duchesne, M. T. Tripodal diglycolamides as highly efficient extractants for f-elements. *New J. Chem.* **2008**, *32*, 490−495. (d) Ansari, S. A.; Mohapatra, P. K.; Verboom, W.; Rao, L. Thermodynamics of biphasic lanthanide extraction by tripodal diglycolamide: a solution calorimetry study. *Dalton Trans.* **2016**, *45*, 17216−17222.

(11) (a) Iqbal, M.; Mohapatra, P. K.; Ansari, S. A.; Huskens, J.; Verboom, W. Preorganization of diglycolamides on the calix[4]arene platform and its effect on the extraction of Am(III)/Eu(III). *Tetrahedron* **2012**, *68*, 7840−7847. (b) Ansari, S. A.; Mohapatra, P. K.; Ali, Sk. M.; Sengupta, A.; Bhattacharyya, A.; Verboom, W. Understanding the complexation of Eu3+ with three diglycolamide-functionalized calix[4]arenes: spectroscopic and DFT studies. *Dalton Trans.* **2016**, *45*, 5425−5429. (c) Huang, H.; Ding, S.; Liu, N.; Wu, Y.; Su, D.; Huang, S. *Sep. Purif. Technol.* **2014**, *123*, 235−240. (d) Ansari, S. A.; Mohapatra, P. K.; Kandwal, P.; Verboom, W. Diglycolamide-Functionalized Calix[4]arene for Am(III) Recovery from Radioactive Wastes: Liquid Membrane Studies Using a Hollow Fiber Contactor. *Ind. Eng. Chem. Res.* **2016**, *55*, 1740−1747.

(12) (a) Li, C. X.; Wu, L.; Chen, L. X.; Yuan, X. Y.; Cai, Y. M.; Feng, W.; Liu, N.; Ren, Y.; Sengupta, A.; Murali, M. S.; Mohapatra, P. K.; Tao, G. H.; Zeng, H. Q.; Ding, S. D.; Yuan, L. H. Highly efficient extraction of actinides with pillar[5]arene-derived diglycolamides in ionic liquids via a unique mechanism involving competitive host−guest interactions. *Dalton Trans.* **2016**, *45*, 19299−19310. (b) Wu, L.; Fang, Y. Y.; Jia, Y. M.; Yang, Y. Y.; Liao, J. L.; Liu, N.; Yang, X. S.; Feng, W.; Ming, J. L.; Yuan, L. H. Pillar[5]arene-based diglycolamides for highly efficient separation of americium(III) and europium(III). *Dalton Trans.* **2014**, *43*, 3835−3838.

(13) (a) Leoncini, A.; Mohapatra, P. K.; Bhattacharyya, A.; Raut, D. R.; Sengupta, A.; Verma, P. K.; Tiwari, N.; Bhattacharyya, D.; Jha, S.; Wouda, A. M.; Huskens, J.; Verboom, W. Unique selectivity reversal in Am^{3+}−Eu^{3+} extraction in a tripodal TREN-based diglycolamide in

DOI: 10.1021/acs.inorgchem.9b00985
Inorg. Chem. 2019, 58, 8633−8644

ionic liquid: extraction, luminescence, complexation and structural studies. *Dalton Trans.* **2016**, *45*, 2476−2484. (b) Mahanty, B.; Ansari, S. A.; Mohapatra, P. K.; Leoncini, A.; Huskens, J.; Verboom, W. Liquid-liquid extraction and facilitated transport of f-elements using an N-pivot tripodal ligand. *J. Hazard. Mater.* **2018**, *347*, 478−485. (c) Mahanty, B.; Satpati, A. K.; Kumar, S.; Leoncini, A.; Huskens, J.; Verboom, W.; Mohapatra, P. K. Evaluation of a novel PVC-based efficient potentiometric sensor containing a tripodal diglycolamide (TREN-DGA) ionophore for europium(III) estimation. *Sens. Actuators, B* **2018**, *272*, 534−542.

(14) Sasaki, Y.; Sugo, Y.; Suzuki, S.; Tachimori, S. The novel extractants, diglycolamides for the extraction of lanthanides and actinides in HNO_3 − n-dodecane system. *Solvent Extr. Ion Exch.* **2001**, *19*, 91−103.

(15) (a) Ali, Sk. M.; Pahan, S.; Bhattacharyya, A.; Mohapatra, P. K. Complexation thermodynamics of diglycolamide with f-elements: solvent extraction and density functional theory analysis. *Phys. Chem. Chem. Phys.* **2016**, *18*, 9816−9828. (b) Ansari, S. A.; Gujar, R. B.; Mohapatra, P. K. Complexation of tetraalkyl diglycolamides with trivalent f-cations in a room temperature ionic liquid: extraction and spectroscopic investigations. *Dalton Trans.* **2017**, *46*, 7584−7593. (c) Kannan, S.; Moody, M. A.; Barnes, C. L.; Duval, P. B. Lanthanum(III) and Uranyl(VI) diglycolamide Complexes: Synthetic Precursors and Structural Studies Involving Nitrate Complexation. *Inorg. Chem.* **2008**, *47*, 4691−4695.

(16) Ellis, R. J.; Brigham, D. M.; Delmau, L.; Ivanov, A. S.; Williams, N. J.; Vo, M. N.; Reinhart, B.; Moyer, B. A.; Bryantsev, V. A. Straining" to Separate the Rare Earths: How the Lanthanide Contraction Impacts Chelation by Diglycolamide Ligands. *Inorg. Chem.* **2017**, *56*, 1152−1160.

(17) Bünzli, J.-C. G.; Mabillard, C.; Yersin, J.-R. FTIR and Fluorometric Investigation of Rare-Earth and Metallic Ion Solvation 0.2. Europium Perchlorate and Nitrate in Anhydrous Solutions Containing Dimethylsulfoxide. *Inorg. Chem.* **1982**, *21*, 4214−4218.

(18) Binnemans, K. Interpretation of europium(III) spectra. *Coord. Chem. Rev.* **2015**, *295*, 1−45.

(19) Barthelemy, P. P.; Choppin, G. R. Luminescence study of complexation of europium and dicarboxylic acids. *Inorg. Chem.* **1989**, *28*, 3354−3357.

(20) Jorgensen, C. K. *Absorption Spectra and Chemical Bonding in Complexes*; Pergamon Press: London, 1962.

(21) Singha Deb, A. K.; Ali, Sk. M.; Shenoy, K. T.; Ghosh, S. K. Adsorption of Eu^{3+} and Am^{3+} ion towards hard donor-based diglycolamic acid-functionalised carbon nanotubes: density functional theory guided experimental verification. *Mol. Simul.* **2015**, *41*, 490−503.

(22) (a) Reed, A. E.; Weinhold, F. Natural bond orbital analysis of near-Hartree−Fock water dimer. *J. Chem. Phys.* **1983**, *78*, 4066−4073. (b) Reed, A. E.; Weinstock, F.; Weinhold, F. Natural population analysis. *J. Chem. Phys.* **1985**, *83*, 735−746. (c) Reed, A. E.; Curtiss, L. A.; Weinhold, F. Intermolecular interactions from a natural bond orbital, donor-acceptor viewpoint. *Chem. Rev.* **1988**, *88*, 899−926.

(23) Mohapatra, P. K.; Iqbal, M.; Raut, D. R.; Verboom, W.; Huskens, J.; Godbole, S. V. Complexation of novel diglycolamide functionalized calix[4]arenes: Unusual extraction behaviour, transport, and fluorescence studies. *Dalton Trans.* **2012**, *41*, 360−363.

(24) *Vogel's Text Book of Quantitative Chemical Analysis*, 5th ed.; Jeffery, G. H.; Bassett, J.; Mendham, J.; Denney, R. C., Eds.; Addison-Wesley Longman Limited: England, 1996; p 329.

(25) Gans, P.; Sabatini, A.; Vacca, A. Investigation of equilibria in solution. Determination of equilibrium constants with the HYPERQUAD suite of programs. *Talanta* **1996**, *43*, 1739−1753.

(26) (a) Becke, A. D. Density-functional thermochemistry. III. The role of exact exchange. *J. Chem. Phys.* **1993**, *98*, 5648−5652. (b) Lee, C.; Yang, W.; Parr, R. G. Development of the Colle-Salvetti correlation-energy formula into a functional of the electron density. *Phys. Rev. B: Condens. Matter Mater. Phys.* **1988**, *37*, 785−789.

(27) Schaefer, A.; Horn, H.; Ahlrichs, R. J. Fully optimized contracted Gaussian basis sets for atoms Li to Kr. *J. Chem. Phys.* **1992**, *97*, 2571−2577.

(28) (a) Ahlrichs, R.; Bar, M.; Haser, M.; Horn, H.; Kolmel, C. Electronic structure calculations on workstation computers: The program system Turbomole. *Chem. Phys. Lett.* **1989**, *162*, 165−169. (b) *TURBOMOLE* V6.0 2009, a development of the University of Karlsruhe and Forschungszentrum Karlsruhe GmbH, TURBOMOLE GmbH, 1989−2007.

(29) (a) Dolg, M.; Stoll, H.; Preuss, H. Energy-adjusted ab initio pseudopotentials for the rare earth elements. *J. Chem. Phys.* **1989**, *90*, 1730−1734. (b) Kuchle, W.; Dolg, M.; Stoll, H.; Preuss, H. Energy-adjusted pseudopotentials for the actinides. Parameter sets and test calculations for thorium and thorium monoxide. *J. Chem. Phys.* **1994**, *100*, 7535−7542. (c) Cao, X.; Dolg, M. Segmented contraction scheme for small-core actinide pseudo-potential basis sets. *J. Mol. Struct.: THEOCHEM* **2004**, *673*, 203−209. (d) Cao, X.; Dolg, M. Segmented contraction scheme for small-core lanthanide pseudopotential basis sets. *J. Mol. Struct.: THEOCHEM* **2002**, *581*, 139−147.

(30) Klamt, A. Conductor-like Screening Model for Real Solvents: A New Approach to the Quantitative Calculation of Solvation Phenomena. *J. Phys. Chem.* **1995**, *99*, 2224−2235.

(31) Shamov, G. A.; Schreckenbach, G.; Vo, T. N. A comparative relativistic DFT and ab initio study on the structure and thermodynamics of the oxofluorides of uranium (IV), (V) and (VI). *Chem. - Eur. J.* **2007**, *13*, 4932−4947.

(32) (a) Ali, Sk. M.; Joshi, J. M.; Singha Deb, A. K.; Boda, A.; Shenoy, K. T.; Ghosh, S. K. Dual mode of extraction for Cs^+ and Na^+ ions with dicyclohexano-18-crown-6 and bis(2-propyloxy)calix[4]-crown-6 in ionic liquids: density functional theoretical investigation. *RSC Adv.* **2014**, *4*, 22911−22925. (b) Ali, Sk. M. Design and screening of suitable ligand/diluent systems for the removal of Sr^{2+} ions from nuclear waste: Density functional theoretical modelling. *Comput. Theor. Chem.* **2014**, *1034*, 38−52. (c) Ali, Sk. M. Thermodynamical Criteria of the Higher Selectivity of Zirconium Oxycations over Hafnium Oxycations towards Organophosphorus Ligands: Density Functional Theoretical Investigation. *Eur. J. Inorg. Chem.* **2014**, *2014*, 1533. (d) Pahan, S.; Boda, A.; Ali, Sk. M. *Theor. Chem. Acc.* **2015**, *134*, 41−57.

(33) (a) Wang, C. Z.; Lan, J. H.; Wu, Q. Y.; Zhao, Y. L.; Wang, X. K.; Chai, Z. F.; Shi, W. Q. nsity functional theory investigations of the trivalent lanthanide and actinide extraction complexes with diglycolamides. *Dalton Trans.* **2014**, *43*, 8713−8720. (b) Justin, J. P.; Sundararajan, M.; Vincent, M. A.; Hiller, I. H. The geometric structures, vibrational frequencies and redox properties of the actinyl coordination complexes ($[AnO_2(L)_n]$ m; An = U, Pu, Np; L = H_2O, Cl^-, CO_3^{2-}, $CH_3CO_2^-$, OH^-) in aqueous solution, studied by density functional theory methods. *Dalton Trans.* **2009**, No. 30, 5902−5909. (c) Manna, D.; Ghanty, T. K. Complexation behavior of trivalent actinides and lanthanides with 1,10-phenanthroline-2,9-dicarboxylic acid based ligands: insight from density functional theory. *Phys. Chem. Chem. Phys.* **2012**, *14*, 11060−11069.

(34) (a) Shamov, G. A.; Schreckenbach, G. Density Functional Studies of Actinyl Aquo Complexes Studied Using Small-Core Effective Core Potentials and a Scalar Four-Component Relativistic Method. *J. Phys. Chem. A* **2005**, *109*, 10961−10974. (b) Boda, A.; Joshi, J. M.; Ali, Sk. M.; Shenoy, K. T.; Ghosh, S. K. *J. Mol. Model.* **2013**, *19*, 5277−5291. (c) Boda, A.; Ali, Sk. M.; Shenoy, K. T.; Ghosh, S. K. Density Functional Theoretical Modeling of Selective Ligand for the Separation of Zr and Hf Metal Oxycations (ZrO^{2+} and HfO^{2+}). *Sep. Sci. Technol.* **2013**, *48*, 2397−2409.

DOI: 10.1021/acs.inorgchem.9b00985
Inorg. Chem. 2019, 58, 8633−8644